Published in final edited form as:
Bioconjug Chem. 2012 August 15; 23(8): 1513–1523. doi:10.1021/bc200606s.

Design and Synthesis of Multifunctional Gold Nanoparticles Bearing Tumor-Associated Glycopeptide Antigens as Potential Cancer Vaccines

Raymond P. Brinas[1], **Andreas Sundgren**[1,2], **Padmini Sahoo**[3], **Susan Morey**[3], **Kate Rittenhouse-Olson**[3], **Greg E. Wilding**[4], **Wei Deng**[4], and **Joseph J Barchi Jr.**[1,*]

[1]Chemical Biology Laboratory, Center for Cancer Research, National Cancer Institute, Frederick National Laboratory for Cancer Research, Frederick, MD 21702

[3]Department of Biotechnical and Clinical Laboratory Sciences, University of Buffalo, Buffalo NY, 14214

[4]Department of Biostatistics, School of Public Health and Health Professions, University of Buffalo, Buffalo NY, 14214

Abstract

The development of vaccines against specific types of cancers will offer new modalities for therapeutic intervention. Here we describe the synthesis of a novel vaccine construction prepared from spherical gold nanoparticles of 3–5 nm core diameters. The particles were coated with both the tumor-associated glycopeptides antigens containing the cell-surface mucin MUC4 with Thomsen Friedenreich (TF) antigen attached at different sites and a 28-residue peptide from the complement derived protein C3d to act as a B-cell activating “molecular adjuvant”. The synthesis entailed solid phase glycopeptide synthesis, design of appropriate linkers and attachment chemistry of the various molecules to the particles. Attachment to the gold surface was mediated by a novel thiol-containing 33 atom linker which was further modified to be included as a third “spacer” component in the synthesis of several three-component vaccine platforms. Groups of mice were vaccinated either with one of the nanoplatform constructs or with control particles without antigen coating. Evaluation of sera from the immunized animals in enzyme immunoassays (EIA) against each glycopeptide antigen showed a small but statistically significant immune response with production of both IgM and IgG isotypes. Vaccines with one carbohydrate antigen (B, C and E) gave more robust responses than the one with two contiguous disaccharides (D), and vaccine E with a TF antigen attached to threonine at the 10th position of the peptide was selected for IgG over IgM suggesting isotype switching. The data suggested that this platform may be a viable delivery system for tumor-associated glycopeptide antigens.

Keywords

gold nanoparticle; tumor-associated carbohydrate antigen; glycopeptides; vaccine

[*]Corresponding Author National Cancer Institute at Frederick 376 Boyles St., PO Box B Bldg. 376, Rm. 209 Frederick, MD 21702. barchi@helix.nih.gov; 301-846-5905 (VOICE) 301-846-6033 (FAX).
[2]Present address: Norwegian Medicines Agency Sven Oftedals vei 8, N-0950 Oslo, Norway + 47 22 89 77 00 (V) + 47 22 89 77 99 (FAX) Andreas.Sundgren@legemiddelverket.no www.legemiddelverket.no

Supporting Information Available: UV-vis spectra of all AuNP constructs, DLS histograms with polydispersity measurements, zeta potential graphs, ^{1}H NMR spectra of all synthetic molecules and AuNP's, and transmission electron microscopy images of AuNP's. This material is available free of charge via the Internet at http://pubs.acs.org.

INTRODUCTION

Tumor-associated carbohydrate antigens(1) (TACA's) are aberrantly expressed glycan chains on cell surface proteins and lipids specific to various tumor subtypes. They arise from the modified expression of various glycoprocessing enzymes in tumors leading to structures that are otherwise rarely observed in the “normal” cell phenotype. Both N- and O-linked glycans, the two major forms of carbohydrate post-translational protein modifications, are modified in specific ways: N-linked (attached to asparagines) glycans become more branched and extended while O-linked (attached to serine/threonine) are truncated and prematurely sialylated. These modifications lead to a variety of cellular consequences within the tumor, including modified cell adhesion, enhanced aggression and metastasis.(2) In addition, the shortened O-linked glycans linked to cell surface proteins called mucins, expose underlying peptide sequences that are masked by heavily clustered glycosylation in normal tissue. This presentation of new sugar chains and amino acid motifs elicits a tumor type-specific immune response against these “non-self” structures.(3) Hence, a variety of studies in the past twenty years have attempted to use TACA's as immunogens for active immunity against different tumors.(4–13) In addition, passive therapy with antibodies directed toward TACA structures such as the Tn(14) and TF(15) antigens also have demonstrated therapeutic potential via inhibition of tumor cell-specific adhesion events.

More importantly, a judicious combination of both the TACA saccharide and the underlying peptide sequence should more accurately present the true antigen to the immune system in a vaccine preparation. Several TACA-containing glycopeptides have been employed in vaccines and immunotherapeutic applications against various tumors.(8, 10–12, 16–33) The majority of these glycopeptides are synthetic in origin, as it is difficult to isolate homogeneous glycosylated protein fragments from cell or tissue preparations. The immune response to these antigens is highly dependent on the chemistry that is used to prepare the vaccine: Differences can be seen with different linkers, carrier proteins, multivalent scaffolds and antigen conformations. Thus, each construct needs to be evaluated on a case-by-case basis and compared with regard to proper presentation of antigen and efficacy in eliciting a response.

We have been interested in employing metal nanoparticles as scaffolds for multivalent presentation of sugars and glycopeptides for various applications.(34–36) In particular, gold nanoparticles (AuNPs) are useful insomuch as they are easily prepared, present a high degree of multivalency and their size range is easily controllable.(37) Several biological applications of carbohydrate-coated gold “glyconanoparticles” (GNP) have been published which attest to the validation of using this simple and highly non-toxic platform.(38) Several years ago, we reasoned that these platforms may be used as carriers of tumor antigens and hence as possible novel vaccine constructs. Since then one article was published on the synthesis of a potential vaccine using carbohydrate-coated gold nanoparticles.(39) Here we present the synthesis of several new gold nanoparticle-based glycopeptides constructions as possible “carriers” for TACA's and TACA-conjugated glycopeptides. The peptide sequences are from MUC4, a biomarker mucin for pancreatic adenocarcinomas(40) and hence a valid starting target for vaccine development.

EXPERIMENTAL SECTION

General Methods

Chemicals were purchased from Aldrich–Sigma (Milwaukee, WI) and used without further purification. $HAuCl_4 \cdot H_2O$ was purchased from Strem Chemicals. The H-Gly-ClTrt resin was purchased from Novabiochem (Darmstadt, Germany). Flash column chromatography (FCC) was performed using RediSep silica columns on a CombiFlash Companion

employing solvent polarity gradient (Dichloromethane→methanol). Preparative reversed phase HPLC was performed using Phenomenex Columbus column (C18, 5 μ, 0.100 Å) employing gradient elutions of varying percent water to organic modifier (solvent A: 0.1% TFA/H2O; solvent B 0.1% TFA/acetonitrile). Analytical reversed-phase chromatography was done using a Phenomenex Gemini column (C18, 5 μ, 110 Å, 150 mm × 4.6 mm) with similar gradients. NMR spectra were recorded on a Varian Inova 400 instrument with residual $CHCl_3$ (7.26 ppm) as the internal standard at frequencies of 399.74 MHz for ^1H and 100.51 MHz for ^{13}C. High resolution mass spectra were performed by Mass Spectrometry Facility at University of California, Riverside.

TEM Measurements

Transmission electron micrographs samples were prepared by placing an aqueous solution (~2μl) of the AuNP's on the grid with a carbon-coated support film that was previously treated with glow discharge. The excess liquid was blotted with a filter paper, allowed to dry, and rinsed with distilled water twice. TEM images were taken using a Hitachi H7650 TEM (Tokyo, Japan) operating at 80 kV with a 2k×2k CCD camera (AMT; Danvers, MA). The sizes of Au NPs were analyzed using the camera's measurement software (AMT).

DLS Measurements

Dynamic Light Scattering measurements were performed on a DynaPro Tytan instrument equipped with a Temperature-Controlled MicroSampler (Wyatt Technology Corp., Santa Barbara, CA) at a laser wavelength of 830 nm, scattering angle of 90° in a 12-μl quartz cuvette at 23°C. Each measurement consisted of sixty 10-second acquisitions. All samples were centrifuged before measurements. To obtain the hydrodynamic radii (R_h) and percentage polydispersity, the intensity autocorrelation functions were fitted with a proprietary non-negative least squares algorithm by *Dynamics 7.0.3* software (Wyatt Technology Corp., Santa Barbara, CA.).

Zeta Potential measurements

A Malvern Zetasizer Nano ZS instrument was used to measure zeta potential at 25° C for all samples. Stock samples were diluted 10-fold in 10 mM NaCl and loaded into pre-rinsed folded capillary cells for measurements. Sample pH was measured before each measurement. An applied voltage of 150 V was used and a minimum of three measurements were made per sample (see Supporting Information for additional descriptions).

Synthesis

N-(-2(2-Hydroxyethylamino)-2-oxoethyl)-1-(7-mercaptoheptanamido)-3,6,9,12,15,18-hexaoxahenicosan-21-amide (6). The hydroxyl linker **6** via the intermediate acid **4** was synthesized by a slightly modified version of our previous synthesis (41) as follows: To a well-stirred solution of the commercially available (PolyPeptides, San Diego, CA) Fmoc-21-amino-4,7,10,13,16,19-hexaoxaheneicosanoic acid (**1**, 200 mg, 0.347 mmol) in dry DMF (1.74 mL) was added HOAt (47.2 mg, 0.347 mmol). After 5 min of stirring, HATU (132 mg, 0.347 mmol) was added and the reaction mixture was stirred for 15 min. H-Gly-2Cl-TrT resin (434 mg of 0.404 mmol/g, 0.175 mmol) was added to the activated acid mixture, followed by diisopropylethylamine (DIEA, 121 μl, 0.694 mmol). After 2 h, the reaction was filtered, and the resin was washed 5 × with DMF. Any remaining amino groups were capped with a 2-Chloro CBz group by reaction with N-(2-Chlorobenzyloxycarbonyloxy)succinimide (Z-(2Cl)-OSu, 394 mg in 2.8 mL 1:1 DMF-DCM). The excess capping reagent solution was filtered, and the resin was washed again with DMF (5×). Based on the Fmoc-group cleavage of a small amount of the resin, the yield of the intermediate **2** was found to be 74%. Resin 2 (470 mg, 0.274 mmol/g, 0.129 mmol)

was deprotected with 4 mL of 20% piperidine in DMF for 1 h at r.t. The mixture was filtered, and the resin was washed with DMF (5×). 7-(Acetylthio)heptanoic acid (31.6 mg, 0.155 mmol) was mixed with HOAt (21 mg, 0.155 mmol) in DMF (0.8 mL). HATU (59 mg, 0.155 mmol) was added, and the mixture was stirred for 5 min. The mixture was added to the deprotected resin, DIEA (54 μl, 40 mg, 0.310 mmol) was added and the mixture was allowed to react for 2 h. The resulting resin **3** was filtered, washed with DMF (5×), DCM (2×), and diethyl ether (2×) and dried under vacuum. This resin **3** (104 mg, 0.159 mg) was cleaved with TFA/thioanisole/water/phenol/EDT (82.5:5:5:5:2.5) for 2 h at r.t. The solvent was evaporated to dryness, the residue was collected, dissolved in water and lyophilized overnight. The crude product was purified by reversed-phase HPLC (A:B, 20% to 50% over 32.7 min) to give the pure **4** in 66.2% yield (51 mg). Compounds **5** and **6** were subsequently prepared according to our previously published procedures. Characterization data of all compounds was in good agreement with the published results.(41)

General Procedure for the Synthesis of the Thiolated Peptides

Peptides were prepared by Fmoc chemistry on a Liberty Microwave Peptide synthesizer (CEM corp., North Carolina, USA). The glyco-amino acids (threonine or serine with an α-O-linked peracetylated Thomsen-Friedenreich disaccharide and Fmoc-protected amino group, TF-Ser, TF-Thr) were either prepared as described(42) or purchased from Sussex Research (Ontario, Canada). The general protocol using the microwave-assisted peptide synthesis is as follows: (1) 0.100 mmol of the resin (Rink amide resin with the first Fmoc-protected amino acid, ~0.35 meq/g substitution) was loaded into the synthesizer; (2) A two-step deprotection sequence was performed; step 1 involved treatment with 20% piperidine in DMF (containing 0.1M HOBt) for 30 s at 75°C (25 W maximum) followed by step 2 which was treatment with a second portion of 20% piperidine in DMF (containing 0.1M HOBt) for 3 min at 75°C (25 W). (3) Coupling reactions were carried out by reacting the resin with four-fold excess of the next amino acid in the presence of HBTU/DIEA for 2 min at 75°C (25 W). Deprotection (step 2) and coupling (step 3) were repeated until the desired peptide sequence was complete. The Fmoc-protected peptide on the resin was then manually deprotected using 20% piperidine in DMF for 1 hour at r.t. in order to couple with either the glycoamino acid or the linker **4** to form the desired peptide. The coupling of each glycoamino acid (1.1 equiv) to the peptide was done manually by activation with HATU (1.1 equiv) and HOAt (1.1 equiv) for 5 min followed by reaction at 25°C for 2 h in the presence of DIPEA (2.2 equiv). Coupling of the linker **4** with the peptides or glycopeptides on the resin was done by standard DIPCDI/HOBt conditions (see Schemes 2 and 3). Briefly, linker **4** was dissolved in DMF, and then HOBt and DIPCDI were added. The resulting mixture was agitated for 30 min at r.t. and added to the resin. After 5–6 h of agitation, another portion of HOBt (5 equiv) and DIPCDI (5 equiv) was added. The mixture was agitated for an additional 18 h. The resin was isolated, washed with DMF (5x) and ethanol (2x), and treated with 10% hydrazine hydrate in EtOH for 18 h. After removal of the hydrazine hydrate solution, the resin was washed with ethanol, DMF and ethyl ether. The resin was dried under vacuum and then treated with the cleavage mixture (2.5% 1,2-ethanedithiol/ 2.5% water/95% TFA) for 2 h. Precipitation of the peptides was done by pouring the TFA solution into a flask containing ice-cold ether. The precipitates were collected by centrifugation. The residue was purified by HPLC (water/acetonitrile gradient, each containing 0.1% TFA) to give the desired peptide as a white, fluffy solid.

HS-Linker-KFLTTAKDKQRWEDPGKQLYQVEATSYA (C3d)

This compound was synthesized in 20% yield (32 mg). RP-HPLC (water/acetonitrile gradient, 15 to 45%, 20 min): R_t=13.3 min. HRMS–ESI (m/z): M^+ calcd for $C_{171}H_{270}N_{42}O_{54}S$, 3807.9388; found: 3807.9241

HS-Linker-TSSAS(Galβ1→3GalNAcα)TGHATPLPVTD (5-TF)

This compound was synthesized in 22% yield (22 mg) RP-HPLC (water/acetonitrile gradient, 15 to 45%, 20 min): R_t = 11.77 min. HRMS–ESI (m/z): M^+ calcd for $C_{102}H_{172}N_{22}O_{44}S$, 2441.1613; found: 2441.1589

HS-Linker-TSSAS(Galβ1→3GalNAcα)T(Galβ1→3GalNAcα)GHATPLPVTD (5,6-TF)

This compound was synthesized in 22% yield (25 mg) RP-HPLC (water/acetonitrile gradient, 15 to 45%, 20 min): R_t = 11.40 min. HRMS–ESI (m/z): M^+ calcd for $C_{116}H_{195}N_{23}O_{54}S$, 2806.2935; found: 2806.2981

General Procedure for the Synthesis of Gold Nanoparticles

To a flask containing water (10 ml/total μmol thiol) was added an aqueous solution of the thiols (1:1:3 molar ratio glycopeptide/C3d/hydroxyl-linker) and 58 mM $HAuCl_4$ (2.75 equiv). The pale yellow solution was cooled to 0°C, and an aqueous solution of $NaBH_4$ (1 mL/total μmol thiol) was added over 10 min. The resulting solution was stirred for 2h at 0°C and then for 16 at r.t. The mixture was concentrated and washed with water (2x) using Centriplus ultrafiltration tubes (MWCO 30kDa). The retentate was lyophilized to give the desired Au NPs as dark purple solids.

Mice immunizations and blood sampling

Vaccination studies were performed in 3 week old female Balb/c mice. Groups of 20 mice were each were vaccinated with one of the six GNP's A-F shown in Figure 2 along with a seventh group that was treated with PBS alone as a control. Mice were immunized subcutaneously with their respective GNP antigen and serum samples were obtained preimmunization and at 2, 4, 6, and 12 week time periods. Serum samples from the mice were obtained using submandibular bleeding prior to immunization and two weeks following each injection. All animal protocols were approved by the institutional animal care and use committee and animals were housed in an ALAC accredited animal facility. The marginal model was used to make pairwise comparisons between test groups and control groups and between different times within each test group to determine statistically significant differences in IgG and IgM titers at significance level $\alpha = 0.05$.

Enzyme Immunoassay

Enzyme-linked immunosorbent assays were performed with the mouse serum samples from different time points against the glycopeptides conjugates used for coating the gold nanoparticles. Immulon HB High-Binding EIA 96-well plates were coated with optimized concentration of 1.25 μg/ml each respective glycopeptides conjugate (Scheme 2) and washed four times with 1X TBS-Brij wash buffer. Mouse sera (100 μl of at 1:100 dilution) was added and IgG and IgM were detected by anti-mouse IgG/alkaline phosphatase or anti-mouse IgM/.horseradish peroxidase systems, respectively according to the manufacturers protocol. The TF antigen-binding monoclonal antibody JAA-F11(15) (1mg/ml Stock Solution) was used as a positive control and 1X-PBS Buffer as a negative control.

Statistical Analysis

The marginal model was used to make pairwise comparisons between test groups and control groups and between different times within each test group to determine statistically significant differences in IgG and IgM titers at significance level, $\alpha = 0.05$.(43) Error bars for EIA assays for the seven sets of 20 mice were calculated with this method and reported as standard error from the mean, which is the standard deviation divided by the square root of the sample size: SD/√n.

RESULTS AND DISCUSSION

Particle Design

Our design is illustrated in Figure 1. A small diameter AuNPs can be coated with various molecular entities in the same reaction by performing the self-assembly in the presence of multiple auro-philic reactants. Thiols are commonly used to conjugate to a metallic gold surface due to affinity of sulfur for gold. Thus, using a variation of the Brust-type procedure,(44, 45) GNP vaccine constructs can be prepared in one pot by reduction of gold salts with sodium borohydride in the presence of different thiols. The reductant serves to both reduce the gold to Au(0) and keep the thiols present in their reduced state for binding to the gold.

Choice of Ligands

The choice of ligands was made based on several criteria. First, the aforementioned importance of aberrant mucins expression and O-linked glycosylation in tumor progression is well established. We reasoned also that neither the carbohydrate or peptide sequence alone would be sufficient for a potent immune response (vide supra). Mucin extracellular domains consist of large strings of tandem repeat peptide sequences of between ~16–22 amino acids, decorated with large numbers of O-linked carbohydrate chains that occur in “clusters”. Hence, we used specific glycopeptides from the mucin tandem repeating unit as antigens to attach to gold. There have been a host of immunological studies with MUC1, a mucin found aberrantly expressed on many prostate and breast tumor lines.(28) However, there has been mounting evidence that another mucin, MUC4, is also a valid biomarker, especially for pancreatic carcinomas.(40) The Kunz group has synthesized several MUC4 based glycopeptides containing various TACAs and T-cell epitopes conjugated together chemically as potential single-component vaccines.(27, 46–49) Thus we chose to follow a similar path and prepare MUC4 glycopeptides with covalently attached TF disaccharides as potential antigens. We chose TF as the carbohydrate antigen since this disaccharide is rarely displayed in normal tissue and its presence has been related to enhanced aggression and metastasis of many solid tumors.(15, 50) The use of nanoparticles as a delivery vehicle offers the opportunity to present antigens, potential T-helper peptides and adjuvants within one entity in a multivalent fashion. In addition, although AuNP cores have been implicated in a small number of studies as harboring some immunostmulant activity in vivo,(51) this core will not present both B-and T-cell epitopes as is the case with many of the various carrier proteins that are used for conjugate vaccines, such as KLH and BSA.

Since carbohydrate antigens are T-cell independent, the standard protocol for vaccine design includes conjugation to a large carrier protein such as KLH or alternatively to small peptides such as the PADRE(52) sequence to elicit T-helper cell production for sustained immunological memory and antibody class switching. Our design concentrated on a B-cell immune response and this dictated our choice of “molecular adjuvant” to add to the system. One of these “adjuvants” used in polysaccharidebased vaccines is the final degradation product of the third component of complement or C3d.(53) C3d binds CR2/CD21 on B-cells enhancing cell activation, and, through simultaneous interaction of antigen with B-cell surface immunoglobulin, activates various pathways that crosstalk to reduce amount of antigen needed for activation and enhance antigen uptake and presentation. The CR2/CD21 binding epitope of C3d was mapped to a 28-residue peptide that was shown by surface plasmon resonance to bind to CR2/CD21 and elicit similar immune responses as full length C3d.(54) In addition, immunization with C3d-conjugated antigen can also increase antibody titers and Th1/Th2 cytokine production in CR2/CD21 knockout mice, suggesting an alternate mechanism of immune stimulation in this system.(55) In this study, it was shown that other peptide regions of C3d can turn on a T-cell mediated response in the absence of CR2/CD21. The versatility of this peptide adjuvant suggested C3d was a judicious choice to

include in our design. We concentrated initially on the 28-residue CR2/CD21-binding motif. The third component of our particle was the linker used to attach the other units to the gold surface. This provided an interstitial random “spacer” to reduce the density of the antigen/adjuvant molecules for better molecular recognition. We designed this conjugate to be “naked” at the terminus that normally displays a biologically active entity (e.g., peptide, glycopeptides,C3d) but to present a common functional group, in our case a free hydroxyl, to maintain water solubility.

Synthesis

The synthesis of the hydroxyl-terminated thiol linker (C in Figure 1) followed a modified version of the procedure by our group(41). Notable differences from our previous synthesis were 1) The first three steps were performed on the solid phase and 2) the coupling agents used for peptide bond formation between the various linker segments were 2-(7-Aza-1H-benzotriazole-1-yl)-1,1,3,3-tetramethyluronium hexafluorophosphate (HATU)/ 1-Hydroxy-7-azabenzotriazole (HOAt) in place of DIPCDI/HOBt. These two changes combined to increase yields and efficiency in all reactions. The HATU/HOAt chemistry was used primarily to reduce the reaction times for the amide couplings to only about 2 h versus 18 h needed for the DIPCDI-mediated coupling. The remaining reactions were similar to those in reference 50 (see Scheme 1).

Peptide/glycopeptide synthesis proceeded under mostly standard conditions, i.e., using Fmoc chemistry on Rink amide resins. Serine and threonine glycoamino acids bearing a single TF antigen (Galβ1–3GalNAc-α-O-Ser/Thr) were either prepared as previously described(42) or purchased commercially (see experimental section) and used for incorporation of the TF antigen into the growing peptide chain. In the case of the unglycosylated MUC4 peptide and one with TF antigen at the 10^{th} position (10-TF), the amino acids were coupled using a microwave-assisted peptide synthesizer (CEM Corp.) with HBTU\DIEA coupling chemistry. In spite of these conditions, coupling of the glycoamino acid to the nascent peptide did not occur for the synthesis of the 10-TF construct E. Instead, performing the coupling reaction manually with only a very slight excess of the glycoamino acid and using a more reactive coupling reagent (HATU) furnished the desired glycopeptide in modest yields. This position is notoriously refractory to efficient coupling, as the preceding amino acid is proline, where the combination of a secondary amino group and the steric bulk of the protected TF disaccharide conspire to slow down the reaction. The 28 residue C3d peptide fragment was prepared in a similar fashion (Scheme 2).

Deprotection of the amino termini of the peptides on the Rink amide resin provided the points of attachment for the thiol-terminated linker **4**. The reaction sequence for this is shown in Scheme 2. Employing the DIPCDI/HOBt coupling condition, the coupling of linker to the peptides on resin afforded the thiol-terminated acetylated glycopeptides which were deprotected both on the sugar hydroxyl groups and the thioacetate on resin by treatment with hydrazine hydrate. Cleavage from the resin and HPLC purification afforded the final glycopeptides-linker-thiol units in yields ranging from 11% to 63%.

The AuNP vaccine constructs were synthesized from various glycopeptides, **C3d**, and the hydroxyl-terminated linker **6** via the sodium borohydride reduction of chloroauric acid in the presence of the thiols. The molar ratio of the thiols used in the synthesis was 1:1:3 (**MUC4** peptide/glycopeptide):(C3d peptide):(linker **6**). Previous work by our group and others has shown that a higher ratio of interstitial linker molecules favors better size distribution and ligand recognition.(41) Also, this may confer better presentation of the glycopeptides and the C3d peptide to the receptors since steric crowding is minimal. Six constructs (A-F) with varying antigens were prepared using the aforementioned procedure (Figure 2). These

constructs were very stable in solution and could be stored at 4°C for months. Samples could be lyophilized and reconstituted several times with no sign of precipitation or flocculation.

Characterization

UV-vis spectra of each nano-construct showed typical plasmon band absorption at ~520 nm with extinction coefficients consistent with particles in this size regime (Supporting Information). TEM measurements showed the average core size of each nanoparticle. The sizes of the Au core ranged primarily from 2.40 – 4.5 nm with two of the constructs (A and F) slightly larger (6.98 and 9.0 nm). This was somewhat curious since both of these constructs contained no carbohydrate modifications. Construct F gave the highest coefficient of variation (CV) (40%), followed by construct A (30%), and compared with the much more reasonable values for constructs B-E (18.8 % –22.7%). Dynamic light scattering experiments showed polydispersity measurements ranged from 21 – 55 %. Although the range is broad and the maximum is somewhat high, the autocorrelation functions of each measurement were consistent with polydispersity within a very narrow size range (see data tables and histograms in Supporting Information). Interestingly, all of the constructs bearing a TF-containing glycopeptide exhibited good CV values and a size range of 2.40 nm to 4.7 nm. At present it is not known why GNP's A and F seemed to be inferior to B-E regarding uniformity and polydispersity. However, one possibility is that the covalently attached sugars prevent inter-particle stacking by blocking non-specific binding of peptide chains on opposing GNP's, a phenomenon that may occur readily in construct A. What remains a mystery are the relatively poor results obtained for construct F, which contains solely the linker as a ligand. A possible explanation is the lack of charge on these particles and the presence of a hydroxyl group that may hydrogen bond via water bridges among different particles. This behavior has been observed previously by us when using a similar strategy for particle preparation: Various thio-linker/$HAuCl_4$ molar ratios to prepare simple particles using compound **5** produced particles of unacceptable quality and uniformity with noticeable aggregation (Sundgren and Barchi, unpublished).

Coverage estimates for gold nanoparticles coated with a single ligand are relatively straightforward.(56) Typical analytical techniques such as thermogravimetric and elemental analyses are usually appropriate for determining the surface coverage of these types of constructs. Others have used very specific and sophisticated methods such as spectroscopy of fluorescently labeled ligands,(57) PCR methods for DNA ligands(58) and X-ray crystallography.(59) However, when passivating ligands are derived from several different molecular families, the estimates become much more complex. This is because most of the analytical tools are designed for single-component species. Analysis of mixed-ligand AuNPs requires differential analysis of each molecular family, which could entail laborious separation steps. There are only a few examples in the literature demonstrating the analysis of mixed-ligand AuNPs. Murray and coworkers made efficient use of ESI mass spectrometry(60), but this method, is limited to the analysis of very small AuNP cores (25 to 38 Au atoms). Another method is by selectively labeling the target ligand on AuNP with a fluorophore and then decomposing the AuNP into fluorophore-labeled “free” ligands, which can be subsequently analyzed by fluorescence spectroscopy. This method may not accurately estimate the ligands because of several factors such as the ease with which the flourophore-ligand reaction occurs and/or steric factors.(61) This method is also only applicable to a specific type of functional group on the ligands.

Due to the lack of a general and robust method for determining the coverage of mixed-ligand AuNPs and also because of the complexity of the structure of our glycopeptide ligands (i.e., presence of a wide range of functional groups), an estimation based on the size of the AuNP core would be appropriate. This type of estimation has been used previously by

Penades and coworkers in determining the approximate number of carbohydrate ligands on AuNPs in the only other study where particles of this nature were prepared.(39) An estimate of ligand coverage was based on calculations of surface gold atoms and starting concentrations of reactants. We have performed a similar analysis and find differential coverage based on the TEM-determined core size and theoretical analysis of the number of surface atoms that can be occupied as comprehensively examined by Hostetler, et al.(62) and Lewis, et al.(63) We assumed that the initial ratio of the ligands used to prepare the AuNPs was the same as the ratio present on the nanoparticles. Table 1 lists the estimates for each ligand on the series of AuNPs prepared. More robust methods are desperately needed for quantitative determination of coverage by ligands of any molecular family, and we are working on methods to perform this analysis (to be reported elsewhere).

Zeta potential measurements were performed on each of the constructs and they are shown in Table 2 and graph from the raw data are shown in Figure S18. Construct A with no sugar is the most negative at nearly −25 mV, and the values tend toward more positive potential as sugars are added to the mucin peptide. Given the complexity of our system, it is difficult to predict the exact mechanism for the change in zeta potential, but the data suggest that the MUC4 peptide/glycopeptides and C3d adsorb to the particle surface with different aptitudes during self assembly. The MUC4 sequence contains one aspartate while C3d has four aspartates and 5 basic residues (four lysines and one arginine). With the hydroxyl linker being neutral, a 1:1 addition of each peptide would have a net zero charge, suggesting that adsorption of the more electropositive C3d may exceed that of MUC4 as the mucin sequence is glycosylated; the diglycosylated construct D being the most “electropositive” of the six particles. There are many other factors involved in zeta potential of each system such as van der Waal's interactions and steric compression. However, the intriguing results may offer qualitative clues into the ligand capacity of multi-component AuNP mixtures.

Vaccinations and Analysis of Antisera

All gold particles described here were used to vaccinate mice and their sera were evaluated for binding to the individual antigens that were coated on the particles. Groups of 20 mice each were vaccinated with all six GNP's A-F shown in Figure 2 along with a seventh group that was treated with PBS alone as a control (Figure 2G). Construct F, which is simply GNP's with the linker unit attached and no glycopeptides nor adjuvant, can be considered as a “control” group'. However, since the chemical linker of many synthetic vaccine constructions have been shown to be immunogenic, it also served as an important vaccine conjugate to identify *in vivo* responses generated to the linker alone. Figure 3 shows the enzyme immunoassay (EIA) results with relative responses of both IgM and IgG in the sera of mice before (preimmune) and 12-weeks after vaccinations of representative constructs B-E. All particle vaccines bearing the TF antigen (B-E) gave small but statistically significant antibody responses (both IgG and IgM) from mice injected subcutaneously at 50 μM particle concentration with boosts every two weeks for 12 weeks. Post-immunization responses were significantly higher than pre-vaccination responses for all four particles, against all conjugates that were tested. Most antisera bound to their respective immunogens, but also with the free peptide and to the linker molecules (self glycopeptide, unglycosylated MUC4 peptide and linker alone, Figure 3), however, greatest responses were to the self antigen. Antigens with single TF substitutions at positions 5 or 6 in the MUC4 repeating unit showed almost equal IgM and IgG production whereas the glycopeptide with a single TF threonine-substitution at position 10 seemed to select for IgG (Figure 3D). Clustering the TF antigen on positions 5 and 6 suppressed the response.

Statistical significance calculated with the marginal mode model(43) ($P < 0.05$) was achieved for several responses. A listing of each of these measurements is shown in Table 3. It is apparent that the peptide sequence is generating a significant response as all AuNPs

with vaccine components (A-E) reacted with MUC4 with statistical significance. Group D, with two contiguous TF disaccharides was the only vaccine construct that did not reach significance for IgG generation when tested against its self structure and the unglycosylated peptide. Neither of the control groups reached any statistical significance to any of the tested molecules in the assays.

The work described here is still preliminary but highly encouraging. Many features of the TF antigen make it an ideal vaccine epitope(64): 1) It is found almost exclusively on carcinomas and not normal tissue(65), 2) In human with cancer, those with lower amounts of anti-TF-antigen antibodies have poorer prognoses than those with low circulating levels and, 3) TF-antigen has a defined and distinct role in metastatic spread of various tumor types(50, 66) and thus active or passive anti-TF therapy could have positive consequences on both tumor growth and metastatic spread as well as overall survival. There have been a host of vaccines prepared based on the TF antigen and many have had positive effects.(64) However, none of these therapeutic strategies has found its way to a clinical setting. In order to progress to a more translationally-relevant therapy, finding the proper vaccine vehicle(carrier) to display antigen in the most biologically relevant presentation while choosing the best antigens and stimulatory molecules will be key to producing a high quality immune response with proper specificity and potency. For this reason, a variety of options need to be explored, and nanoparticle carriers are reasonable choices for reasons already discussed. We have prepared various presentations of the TF antigen on gold particles and have tested some of these in mice for immune responses (Barchi and Rittenhouse-Olson, unpublished); however, the constructions described here with the C3d molecular adjuvant were the only ones that gave measureable and statistically significant responses. The provocative differential response of the various structures bodes well for future studies using similar platforms with second generation epitopes and nanopaltforms. These studies are currently in progress and will be reported in due course.

CONCLUSIONS

Several putative glycopeptide antigens were coated onto gold with a molecular adjuvant in defined densities, resulting in particles that could act as both immunogen and immune system stimulant. The preparation of these fully synthetic GNP constructs encompassed 1) Design of appropriate immunogens, 2) Choice of molecular adjuvant and 3) Design of robust linker. Synthesis of the particles proceeded without incident to afford multifunctional GNP's. Characterization showed some constructs were more polydispersed than others, with the linker-coated “control” particles interestingly being the least homogeneous. This is in contrast to our previous particles where shorter linkers were actually the least polydispersed among GNP's with various saccharides.(34) Constructs were prepared with the antigen, molecular adjuvant and interstitial linker coated in a 1:1:3 ratio and there was evidence of differential coating. A response in mice was generated to each glycopeptide antigen with statistical significance; this is one of the first reports of an immune response generated to an immunogen coated on gold without the use of additional adjuvants admixed with the vaccine preparation. Further development to enhance the uniformity and immunogenicity of the particles is in progress. These initial data suggest that glycopeptides-bearing nanoparticles have potential to be part of the repertoire of anticancer vaccine modalities that may have distinct and intriguing therapeutic utility. Details of the comprehensive biological evaluation of these novel particles will be reported in separate publications.

Supplementary Material

Refer to Web version on PubMed Central for supplementary material.

Acknowledgments

The authors wish to acknowledge Sergey Tarasov and Marzena Dyba of the Biophysics Resource, Structural Biophysics Laboratory, NCI Frederick for help in obtaining DLS data and Kunio Nagashima of the Electron Microscopy Laboratory, Advanced Technology Program, NCI Frederick for TEM images. The intramural Research Program of the Center for Cancer Research, National Cancer Institute is acknowledged for financial support.

References

(1). Hakomori SI. Aberrant Glycosylation in Tumors and Tumor-Associated Carbohydrate Antigens. Advances in Cancer Research. 1989; 52:257–331. [PubMed: 2662714]

(2). Dennis JW, Granovsky M, Warren CE. Glycoprotein glycosylation and cancer progression. Biochimica Et Biophysica Acta-General Subjects. 1999; 1473:21–34.

(3). Hanisch FA. O-glycosylation of the mucin type. Biological Chemistry. 2001; 382:143–149. [PubMed: 11308013]

(4). Xu YF, Sette A, Sidney J, Gendler SJ, Franco A. Tumor-associated carbohydrate antigens: A possible avenue for cancer prevention. Immunology and Cell Biology. 2005; 83:440–448. [PubMed: 16033540]

(5). Newsom-Davis TE, Wang D, Steinman L, Chen PFT, Wang LX, Simon AK, Screaton GR. Enhanced Immune Recognition of Cryptic Glycan Markers in Human Tumors. Cancer Research. 2009; 69:2018–2025. [PubMed: 19223535]

(6). Brockhausen I. Glycodynamics of mucin biosynthesis in gastrointestinal tumor cells. Glycobiology and Medicine. 2003; 535:163–188.

(7). Indar A, Maxwell-Armstrong CA, Durrant LG, Carmichael J, Scholefield JH. Current concepts in immunotherapy for the treatment of colorectal cancer. Journal of the Royal College of Surgeons of Edinburgh. 2002; 47:458–474. [PubMed: 12018689]

(8). Cipolla L, Peri F, Airoldi C. Glycoconjugates in cancer therapy. Anti-Cancer Agents in Medicinal Chemistry. 2008; 8:92–121. [PubMed: 18220509]

(9). Slovin SF, Ragupathi G, Musselli C, Fernandez C, Diani M, Verbel D, Danishefsky S, Livingston P, Scher HI. Thomsen-Friedenreich (TF) antigen as a target for prostate cancer vaccine: clinical trial results with TF cluster (c)-KLH plus QS21 conjugate vaccine in patients with biochemically relapsed prostate cancer. Cancer Immunology Immunotherapy. 2005; 54:694–702.

(10). Lo-Man R, Vichier-Guerre S, Perraut R, Deriaud E, Huteau V, BenMohamed L, Diop OM, Livingston PO, Bay S, Leclerc C. A fully synthetic therapeutic vaccine candidate targeting carcinoma-associated Tn carbohydrate antigen induces tumor-specific antibodies in nonhuman primates. Cancer Research. 2004; 64:4987–4994. [PubMed: 15256473]

(11). Buskas T, Ingale S, Boons GJ. Towards a fully synthetic carbohydrate-based anticancer vaccine: Synthesis and immunological evaluation of a lipidated glycopeptide containing the tumor-associated Tn antigen. Angewandte Chemie-International Edition. 2005; 44:5985–5988.

(12). Ingale S, AWolfert M, Gaekwad J, Buskas T, Boons GJ. Robust immune responses elicited by a fully synthetic three-component vaccine. Nature Chemical Biology. 2007; 3:663–667.

(13). Buskas T, Thompson P, Boons GJ. Immunotherapy for cancer: synthetic carbohydrate-based vaccines. Chemical Communications. 2009:5335–5349. [PubMed: 19724783]

(14). Danussi C, Coslovi A, Campa C, Mucignat MT, Spessotto P, Uggeri F, Paoletti S, Colombatti A. A newly generated functional antibody identifies Tn antigen as a novel determinant in the cancer cell-lymphatic endothelium interaction. Glycobiology. 2009; 19:1056–1067. [PubMed: 19528665]

(15). Heimburg J, Yan J, Morey S, Glinskii OV, Huxley VH, Wild L, Klick R, Roy R, Glinsky VV, Rittenhouse-Olson K. Inhibition of spontaneous breast cancer metastasis by anti-Thomsen-Friedenreich antigen monoclonal antibody JAA-F11. Neoplasia. 2006; 8:939–948. [PubMed: 17132226]

(16). Koganty RR, Reddish MA, Longenecker BM. Glycopeptide- and carbohydrate-based synthetic vaccines for the immunotherapy of cancer. Drug Discovery Today. 1996; 1:190–198.

(17). Bay S, LoMan R, Osinaga E, Nakada H, Leclerc C, Cantacuzene D. Preparation of a multiple antigen glycopeptide (MAG) carrying the Tn antigen - A possible approach to a synthetic carbohydrate vaccine. Journal of Peptide Research. 1997; 49:620–625. [PubMed: 9266491]

(18). Kuduk SD, Schwarz JB, Chen XT, Glunz PW, Sames D, Ragupathi G, Livingston PO, Danishefsky SJ. Synthetic and immunological studies on clustered modes of mucin-related Tn and TF O-linked antigens: The preparation of a glycopeptide-based vaccine for clinical trials against prostate cancer. Journal of the American Chemical Society. 1998; 120:12474–12485.

(19). Hilaire PMS, Cipolla L, Franco A, Tedebark U, Tilly DA, Meldal M. Synthesis of T-antigen-containing glycopeptides as potential cancer vaccines. Journal of the Chemical Society-Perkin Transactions. 1999; 1:3559–3564.

(20). Vichier-Guerre S, Lo-Man R, Bay S, Deriaud E, Nakada H, Leclerc C, Cantacuzene D. Short synthetic glycopeptides successfully induce antibody responses to carcinoma-associated Tn antigen. Journal of Peptide Research. 2000; 55:173–180. [PubMed: 10784033]

(21). Kudryashov V, Glunz PW, Williams LJ, Hintermann S, Danishefsky SJ, Lloyd KO. Toward optimized carbohydrate-based anticancer vaccines: Epitope clustering, carrier structure, and adjuvant all influence antibody responses to Lewis(y) conjugates in mice. Proceedings of the National Academy of Sciences of the United States of America. 2001; 98:3264–3269. [PubMed: 11248067]

(22). Kunz H. Synthetic glycopeptides for the development of tumour-selective vaccines. Journal of Peptide Science. 2003; 9:563–573. [PubMed: 14552419]

(23). Vichier-Guerre S, Lo-Man R, BenMohamed L, Deriaud E, Kovats S, Leclerc C, Bay S. Induction of carbohydrate specific antibodies in HLA-DR transgenic mice by a synthetic glycopeptide: a potential anti cancer vaccine for human use. Journal of Peptide Research. 2003; 62:117–124. [PubMed: 12895273]

(24). Xu YF, Gendler SJ, Franco A. Designer glycopeptides for cytotoxic T cell-based elimination of carcinomas. Journal of Experimental Medicine. 2004; 199:707–716. [PubMed: 14993254]

(25). Vichier-Guerre S, Lo-Man R, Huteau V, Deriaud E, Leclerc C, Bay S. Synthesis and immunological evaluation of an antitumor neoglycopeptide vaccine bearing a novel homoserine Tn antigen. Bioorganic & Medicinal Chemistry Letters. 2004; 14:3567–3570. [PubMed: 15177475]

(26). Dziadek S, Kowalczyk D, Kunz H. Synthetic vaccines consisting of tumor-associated MUC1 glycopeptide antigens and bovine serum albumin. Angewandte Chemie-International Edition. 2005; 44:7624–7630.

(27). Dziadek S, Hobel A, Schmitt E, Kunz H. A fully synthetic vaccine consisting of a tumor-associated glycopeptide antigen and a T-Cell epitope for the induction of a highly specific humoral immune response. Angewandte Chemie-International Edition. 2005; 44:7630–7635.

(28). Liakatos A, Kunz H. Synthetic glycopeptides for the development of cancer vaccines. Current Opinion in Molecular Therapeutics. 2007; 9:35–44. [PubMed: 17330400]

(29). Niederhafner P, Reinis M, Sebestik J, Jezek J. Glycopeptide dendrimers, Part III - a review: Use of glycopeptide dendrimers in immunotherapy and diagnosis of cancer and viral diseases. Journal of Peptide Science. 2008; 14:556–587. [PubMed: 18275089]

(30). Westerlind U, Hobel A, Gaidzik N, Schmitt E, Kunz H. Synthetic vaccines consisting of tumor-associated MUC1 glycopeptide antigens and a T-cell epitope for the induction of a highly specific humoral immune response. Angewandte Chemie-International Edition. 2008; 47:7551–7556.

(31). Zhu JL, Wan Q, Ragupathi G, George CM, Livingston PO, Danishefsky SJ. Biologics through Chemistry: Total Synthesis of a Proposed Dual-Acting Vaccine Targeting Ovarian Cancer Orchestration of Oligosaccharide and Polypeptide Domains. Journal of the American Chemical Society. 2009; 131:4151–4158. [PubMed: 19253940]

(32). Ryan SO, Vlad AM, Islam K, Gariepy J, Finn OJ. Tumor-associated MUC1 glycopeptide epitopes are not subject to self-tolerance and improve responses to MUC1 peptide epitopes in MUC1 transgenic mice. Biological Chemistry. 2009; 390:611–618. [PubMed: 19426130]

(33). Brooks CL, Schietinger A, Borisova SN, Kufer P, Okon M, Hirama T, MacKenzie CR, Wang LX, Schreiber H, Evans SV. Antibody recognition of a unique tumor-specific glycopeptide

antigen. Proceedings of the National Academy of Sciences of the United States of America. 2010; 107:10056–10061. [PubMed: 20479270]

(34). Svarovsky SA, Szekely Z, Barchi JJ. Synthesis of gold nanoparticles bearing the Thomsen-Friedenreich disaccharide: a new multivalent presentation of an important tumor antigen. Tetrahedron-Asymmetry. 2005; 16:587–598.

(35). Barchi JJ. Carbohydrate nanoscience: A new realm for biochemical and therapeutic applications. Abstracts of Papers of the American Chemical Society. 2005; 229:U254–U254.

(36). Sundgren A, Barchi JJ. Varied presentation of the Thomsen-Friedenreich disaccharide tumor-associated carbohydrate antigen on gold nanoparticles. Carbohydrate Research. 2008; 343:1594–1604. [PubMed: 18502409]

(37). De la Fuente JM, Penades S. Glyconanoparticles: Types, synthesis and applications in glycoscience, biomedicine and material science. Biochimica Et Biophysica Acta-General Subjects. 2006; 1760:636–651.

(38). Goodman CM, McCusker CD, Yilmaz T, Rotello VM. Toxicity of gold nanoparticles functionalized with cationic and anionic side chains. Bioconjugate Chemistry. 2004; 15:897–900. [PubMed: 15264879]

(39). Ojeda R, de Paz JL, Barrientos AG, Martin-Lomas M, Penades S. Preparation of multifunctional glyconanoparticles as a platform for potential carbohydrate-based anticancer vaccines. Carbohydrate Research. 2007; 342:448–459. [PubMed: 17173881]

(40). Moniaux N, Andrianifahanana M, Brand RE, Batra SK. Multiple roles of mucins in pancreatic cancer, a lethal and challenging malignancy. British Journal of Cancer. 2004; 91:1633–1638. [PubMed: 15494719]

(41). Sundgren A, Barchi J, J. J. Carbohydrate Res. 2008; 343:1594–1604.

(42). Svarovsky SA, Barchi JJ. Highly efficient preparation of tumor antigen-containing glycopeptide building blocks from novel pentenyl glycosides. Carbohydrate Research. 2003; 338:1925–1935. [PubMed: 14499569]

(43). Heagerty PJ, Zeger SL. Marginalized multilevel models and likelihood inference. Statistical Science. 2000; 15:1–19.

(44). Brust M, Walker M, Bethell D, Schiffrin DJ, Whyman R. Synthesis of Thiol-Derivatized Gold Nanoparticles in a 2-Phase Liquid-Liquid System. Journal of the Chemical Society-Chemical Communications. 1994:801–802.

(45). Brust M, Fink J, Bethell D, Schiffrin DJ, Kiely C. Synthesis and Reactions of Functionalized Gold Nanoparticles. Journal of the Chemical Society-Chemical Communications. 1995:1655–1656.

(46). Brocke C, Kunz H. Synthetic glycopeptides of the tandem repeat sequence of the epithelial mucin MUC4 with tumour-associated carbohydrate antigens. Synlett. 2003:2052–2056.

(47). Dziadek S, Brocke C, Kunz H. Biomimetic synthesis of the tumor-associated (2,3)-sialyl-T antigen and its incorporation into glycopeptide antigens from the mucins MUC1 and MUC4. Chemistry-a European Journal. 2004; 10:4150–4162.

(48). Brocke C, Kunz H. Synthetic tumor-associated glycopeptide antigens from the tandem repeat sequence of the epithelial mucin MUC4. Synthesis-Stuttgart. 2004:525–542.

(49). Becker T, Kaiser A, Kunz H. Synthesis of Dendrimeric Tumor-Associated Mucin-Type Glycopeptide Antigens. Synthesis-Stuttgart. 2009:1113–1122.

(50). Glinsky VV, Glinsky GV, Rittenhouse-Olson K, Huflejt ME, Glinskii OV, Deutscher SL, Quinn TP. The role of Thomsen-Friedenreich antigen in adhesion of human breast and prostate cancer cells to the endothelium. Cancer Research. 2001; 61:4851–4857. [PubMed: 11406562]

(51). Zolnik BS, Gonzalez-Fernandez A, Sadrieh N, Dobrovolskaia MA. Minireview: Nanoparticles and the Immune System. Endocrinology. 2010; 151:458–465. [PubMed: 20016026]

(52). Alexander J, del Guercio MF, Maewal A, Qiao L, Fikes J, Chesnut RW, Paulson J, Bundle DR, DeFrees S, Sette A. Linear PADRE T helper epitope and carbohydrate B cell epitope conjugates induce specific high titer IgG antibody responses. Journal of Immunology. 2000; 164:1625–1633.

(53). Toapanta FR, Ross TM. Complement-mediated activation of the adaptive immune responses - Role of C3d in linking the innate and adaptive immunity. Immunologic Research. 2006; 36:197–210. [PubMed: 17337780]

(54). Sarrias MR, Franchini S, Canziani G, Argyropoulos E, Moore WT, Sahu A, Lambris JD. Kinetic analysis of the interactions of complement receptor 2 (CR2, CD21) with its ligands C3d, iC3b, and the EBV glycoprotein gp350/220. Journal of Immunology. 2001; 167:1490–1499.

(55). Knopf PM, Rivera DS, Hai SH, McMurry J, Martin W, De Groot AS. Novel function of complement C3d as an autologous helper T-cell target. Immunology and Cell Biology. 2008; 86:221–225. [PubMed: 18180801]

(56). Srinivasan B, Huang XF. Functionalization of magnetic nanoparticles with organic molecules: Loading level determination and evaluation of linker length effect on immobilization. Chirality. 2008; 20:265–277. [PubMed: 17568438]

(57). Demers LM, Mirkin CA, Mucic RC, Reynolds RA, Letsinger RL, Elghanian R, Viswanadham G. A fluorescence-based method for determining the surface coverage and hybridization efficiency of thiol-capped oligonucleotides bound to gold thin films and nanoparticles. Anal. Chem. 2000; 72:5535–5541. [PubMed: 11101228]

(58). Pease LF, Tsai DH, Zangmeister RA, Zachariah MR, Tarlov MJ. Quantifying the surface coverage of conjugate molecules on functionalized nanoparticles. J. Phys. Chem. C. 2007; 111:17155–17157.

(59). Heaven MW, Dass A, White PS, Holt KM, Murray RW. Crystal structure of the gold nanoparticle [N(C8H17)(4)][Au-25(SCH2CH2Ph)(18)]. J. Am. Chem. Soc. 2008; 130:3754–+. [PubMed: 18321116]

(60). Tracy JB, Kalyuzhny G, Crowe MC, Balasubramanian R, Choi JP, Murray RW. Poly(ethylene glycol) ligands for high-resolution nanoparticle mass spectrometry. J. Am. Chem. Soc. 2007; 129:6706–6707. [PubMed: 17477534]

(61). Maus L, Spatz JP, Fiammengo R. Quantification and Reactivity of Functional Groups in the Ligand Shell of PEGylated Gold Nanoparticles via a Fluorescence-Based Assay. Langmuir. 2009; 25:7910–7917. [PubMed: 19419188]

(62). Hostetler MJ, Wingate JE, Zhong CJ, Harris JE, Vachet RW, Clark MR, Londono JD, Green SJ, Stokes JJ, Wignall GD, Glish GL, Porter MD, Evans ND, Murray RW. Alkanethiolate gold cluster molecules with core diameters from 1.5 to 5.2 nm: Core and monolayer properties as a function of core size. Langmuir. 1998; 14:17–30.

(63). Lewis DJ, Day TM, MacPherson JV, Pikramenou Z. Luminescent nanobeads: attachment of surface reactive Eu(III) complexes to gold nanoparticles. Chemical Communications. 2006:1433–1435. [PubMed: 16550291]

(64). Almogren A, Abdullah J, Ghapure K, Ferguson K, Glinsky VV, Rittenhouse-Olson K. Anti-Thomsen-Friedenreich-Ag (anti-TF-Ag) potential for cancer therapy. Front Biosci (Schol Ed). 2012; 4:840–863. [PubMed: 22202095]

(65). Springer GF. T and Tn Pancarcinoma Markers - Autoantigenic Adhesion Molecules in Pathogenesis, Prebiopsy Carcinoma-Detection, and Long-Term Breast-Carcinoma Immunotherapy. Critical Reviews in Oncogenesis. 1995; 6:57–85. [PubMed: 8573608]

(66). Yu LG. The oncofetal Thomsen-Friedenreich carbohydrate antigen in cancer progression. Glycoconjugate Journal. 2007; 24:411–420. [PubMed: 17457671]

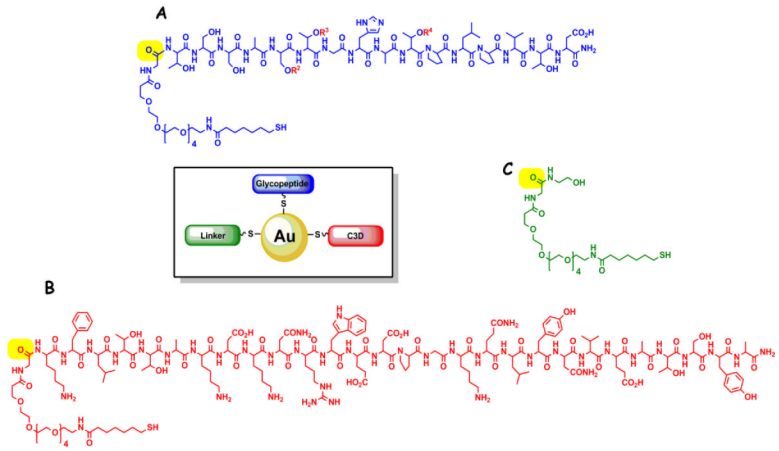

Figure 1.

AuNP vaccine design (center). (A) MUC4 glycopeptides conjugated to the carbonyl highlighted in yellow of the linker shown in (C). R^2-R^4 indicate residues that are glycosylated. (B) C3d 28 residue peptide (P28) conjugated to the linker. The linker in (C) is shown modified with the addition of terminal hydroxyl group to maintain bioavailability and reduce density. The ratio of each thiol used in the construction of AuNPs was **A**:**B**:**C** = 1:1:3

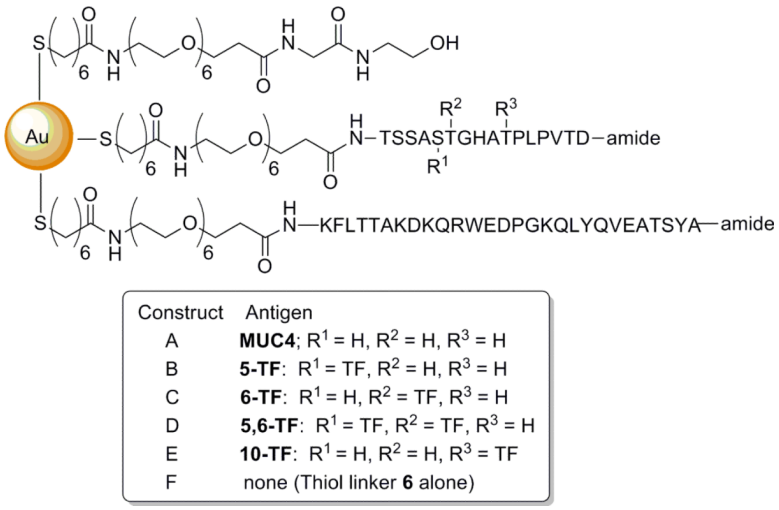

Construct	Antigen
A	**MUC4**; R^1 = H, R^2 = H, R^3 = H
B	**5-TF**: R^1 = TF, R^2 = H, R^3 = H
C	**6-TF**: R^1 = H, R^2 = TF, R^3 = H
D	**5,6-TF**: R^1 = TF, R^2 = TF, R^3 = H
E	**10-TF**: R^1 = H, R^2 = H, R^3 = TF
F	none (Thiol linker **6** alone)

Figure 2.
Structures of the six AuNP-based vaccine constructs prepared in the text.

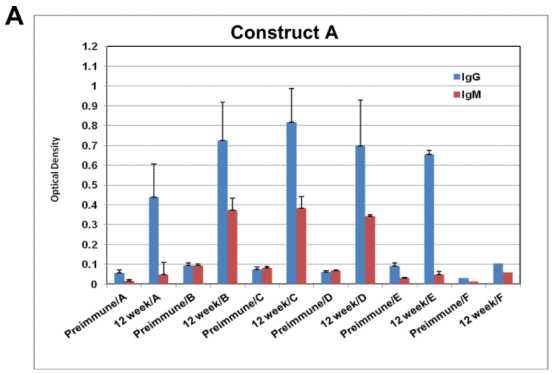

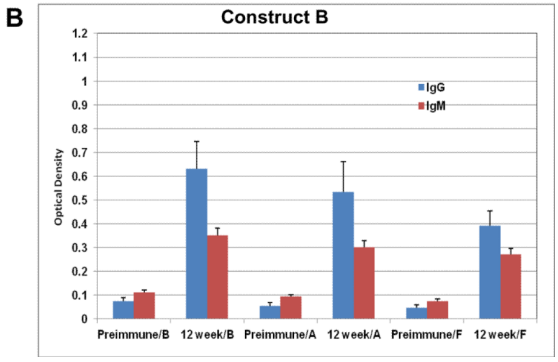

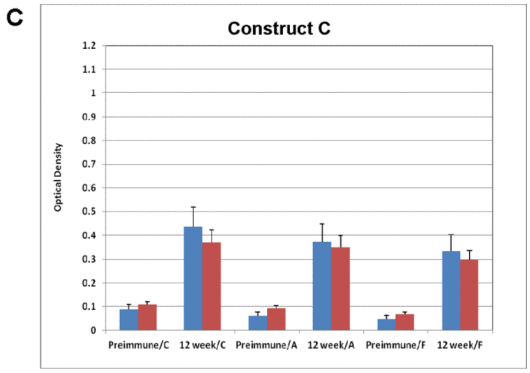

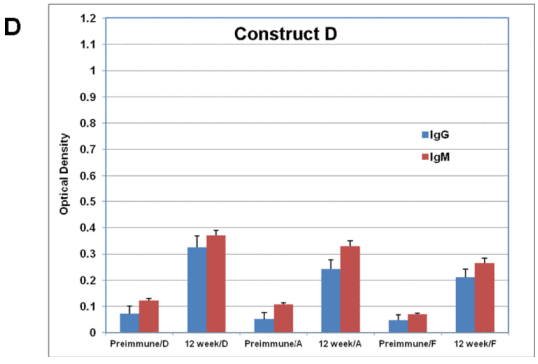

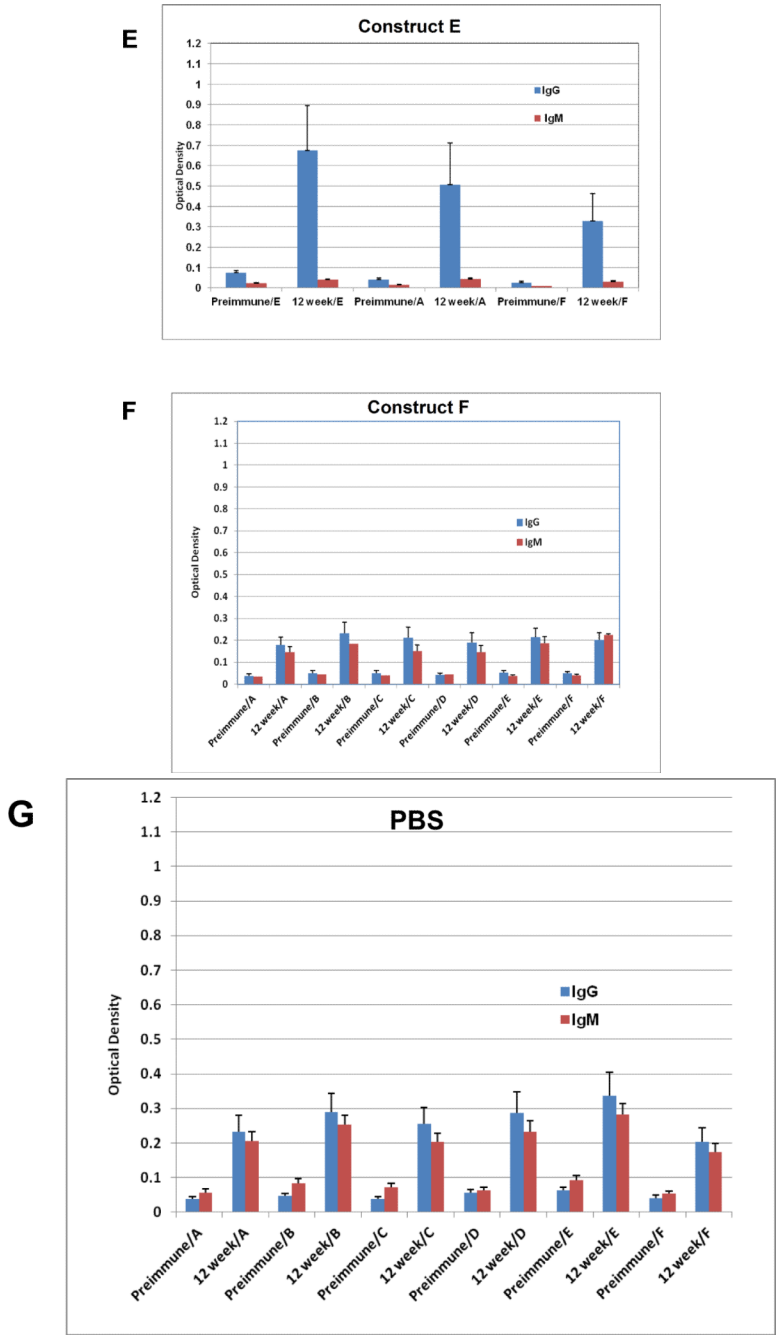

Figure 3.

EIA graphs of sera from mice vaccinated with (A) construct **A** (MUC4); (B) construct **B** (5-TF); (C) construct **C** (6-TF); (D) construct **D** (5,6-TF); (E) construct **E** (10-TF); (F) Construct **F** (linker alone) and G) PBS. The graphs are divided into sets of bars where red [■] represents IgM responses and [■] represents IgG response. Preimmune bleeds are in alternate columns followed by responses after 12 weeks to either self peptide, unglycosylated MUC4 peptide or linker alone for constructs B, C, D and E. For vaccination with the unglycosylated MUC4 peptide (A), linker alone (F) and PBS (G) responses at preimmune and 12-week stages are shown for all constructs.

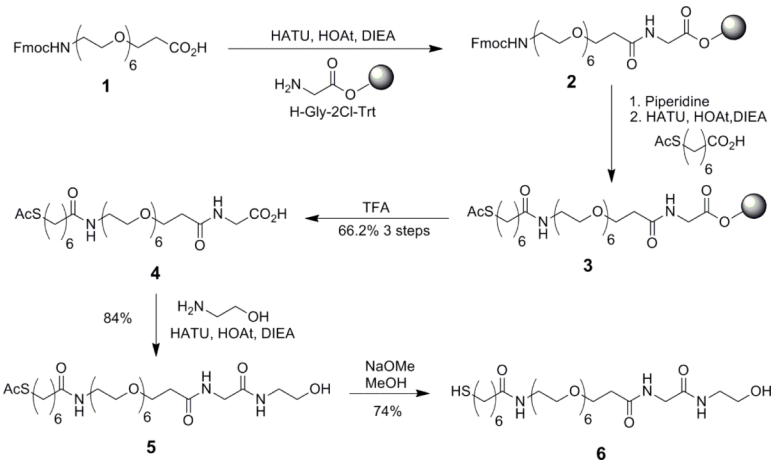

Scheme 1.
Synthesis of the linker with modifications from previous preparations.

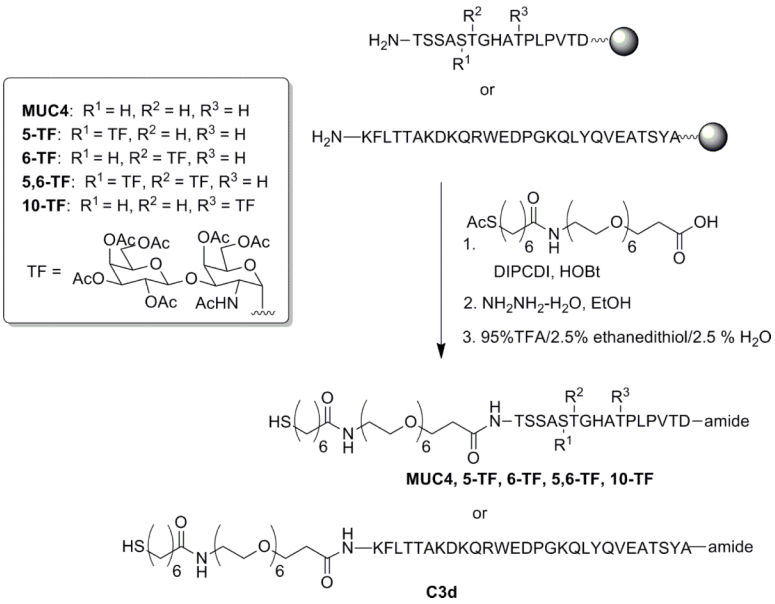

Scheme 2.
Final synthesis of glycopeptides precursors for GNP preparations.

Table 1

Calculated number of antigens and C3d molecules based on the TEM core size of the constructs.

Construct	Core diameter (nm)	Core radius (nm)	Percent Coverage[a]	Number of surface Atoms[b]	Number of thiolate chains[c]	Antigen or C3d Number[d]
A	4.82	2.41	42%	1238	520	104
B	4.70	2.35	42%	1177	494	99
C	3.35	1.68	46%	602	277	55
D	3.28	1.64	46%	573	264	53
E	2.40	1.20	50%	307	154	31
F	9.02	4.51	~33%	4335	1431	-

[a]Based on the calculated percent coverage from reference 53. The value for construct F is the theoretical coverage for large clusters.

[b]The values were calculated using the equations in reference 54.

[c]Obtained by multiplying the number of surface atoms with the percent coverage.

[d]Based on the molar ratio of antigen to C3d to linker during the synthesis, which is 1:1:3.

Table 2

Zeta potential of vaccine constructs.

Vaccine #	pH	Zeta Potential, mV[a]
A	6.3	−24.9 (1.4)
B	6.8	−21.7 (1.0)
C	6.7	−18.4 (2.5)
D	6.9	−13.6 (3.1)
E	7.0	−15.6 (0.8)
F	7.3	−17.4 (0.8)

[a]All measurements were 0.2 mg/ml, in 10 mM NaCl, 25°C. Results are based on an average of three measurements and the values in parentheses represents the standard error.

Table 3

Summary of statistically significant immune responses to AuNP vaccinations.

Group Sera Tested	Molecule Tested Against					
	Self Glycopeptide[a]		MUC4 Peptide[b]		Self and MUC4 Peptide[c]	
	IgG (Pre/12wk)[c]	IgM (Pre/12wk)	IgG (Pre/12wk)	IgM (Pre/12wk)	IgG Self vs MUC-4	IgM Self vs MUC-4
Group A	ND	ND	+	+	ND	ND
Group B	+	+	+	+	+	+
Group C	+	+	+	+	+	+
Group D	-	+	-	+	+	+
Group E	+	+	+	+	+	+
Group F*	-	-	-	-	-	-
Group G*	-	-	-	-	-	-

[a] These columns show responses when each construct was tested against the *glyco*peptides of groups B, C, D and E. A "+" sign indicates statistical significance between sera from mice collected preimmunization and after 12 weeks with $P \leq 0.05$.

[b] Sera from each group was tested against the unglycosylated peptide. Sera from mice vaccinated with all (glyco)peptide-coated AuNPs (A–E) reacted with MUC4 peptide sequence and were statistically significant.

[c] These two columns show that reaction of a specific group sera to the "self" glycopeptides was significantly greater than reaction with the unglycosylated MUC4 peptide for both IgG and IgM. NA= Not determined.